Seasonal and spatial variations in the partial pressure of carbon dioxide in a eutrophic brackish lake, Lake Hamana, Japan

Seasonal and spatial variations in the partial pressure of carbon dioxide in a eutrophic brackish lake, Lake Hamana, Japan

Atsushi Kubo[1*], Keisuke Yoshida[1], Kei Suzuki[1]

Atsushi Kubo (*corresponding author)
E-mail: kubo.atsushi@shizuoka.ac.jp
Tel. +81-54-238-4794

[1]Department of Geosciences, Shizuoka University, 836 Ohya, Suruga-ku, Shizuoka, 422-8529, Japan

Keywords: pCO_2; dissolved oxygen; apparent oxygen utilization; eutrophication; sewage treatment plant

Abstract

The dissolved inorganic carbon and total alkalinity in the surface brackish waters of Lake Hamana were investigated monthly from October 2017 to September 2019 at 14 stations. The partial pressure of carbon dioxide (pCO_2) in the surface water ranged from 29 to 1476 μatm and was undersaturated for atmospheric CO_2 during the observation periods, although most coastal waters were net source areas because of the large amount of terrestrial organic and inorganic carbon input. Since there was a strong negative correlation between pCO_2 and the dissolved oxygen, seasonal and temporal variations in pCO_2 were mainly derived from phytoplankton activity. The high phytopkankton activity induced by the effluents from sewage treatment plants, which was low in carbon and high in nitrogen. Therefore, in urbanized coastal waters with sewage treatment plants, such as the coastal waters of Japan, there is a possibility of shifting from weaker carbon dioxide source areas to sink areas. However, pCO_2 was oversaturated at the polluted river mouth, especially after high precipitation events due to the large carbon supply.

1. Introduction

Globally, coastal waters are regarded as a significant net source of carbon dioxide (CO_2) to the atmosphere because of terrestrial inorganic and organic carbon input (Frankignoulle et al. 1998; Chen et al. 2013; Hotchkiss et al. 2015). Annual CO_2 emissions from coastal waters to the atmosphere are currently estimated to be 0.1–0.5 PgC, which was reported to be approximately 30% of the maximum CO_2 absorption in the open ocean (Chen and Borges 2009; Borges and Abril 2011; Chen et al. 2013). However, there is a possibility that coastal waters, which are affected by intense human activities, are net sinks for CO_2 (Kuwae et al. 2016; Kuwae et al. 2017). Several coastal waters have been reported to be a net sink for atmospheric CO_2 from recent observations (Aby Lagoon, Kone et al. 2009; Guanabara Bay, Cotovicz et al. 2015, 2019; Tokyo Bay, Kubo et al. 2017). Aby Lagoon has a narrow and shallow entrance to the bay and maintains a stratified structure throughout the year. Therefore, organic matter derived from primary production at the surface layer is efficiently transported to the bottom layer. Guanabara Bay and Tokyo Bay have a stratified structure during summer, and the organic matter produced by phytoplankton activities is transported to the bottom layer. In addition, primary production is enhanced due to high nutrient concentrations. Tokyo Bay has a relatively large amount of nutrients flowing into the bay because of the removal of a large amount of organic carbon from the sewage treatment plant (STP) in the basin (Kubo et al. 2017; Kubo and Kanda 2020). As a result, CO_2 consumption from active phytoplankton activity exceeds the effect of CO_2 generation by terrestrial organic matter decomposition. Due to the above mechanism, some coastal waters work as a net sink area for atmospheric CO_2. However, seasonal variations in CO_2 in eutrophic coastal waters have not been mainly observed throughout the year (e.g., Lin et al. 2019; Li et al. 2020).

Global warming has enhanced thermal stratification in the water column (Coma et al. 2009; Breitburg et al. 2018). This enhanced stratification is responsible for the exhaustion of nutrients and blooming of phytoplankton in surface water. Furthermore, the organic matter sinking rate has increased. As a result, the net sink area for atmospheric CO_2 may increase in coastal waters. Moreover, 40% of the world's population lives along the coast. In the future, the individuals that live in coastal areas are expected to increase with STP coverage and sewage treatment efficiency. Recently, Brauko et al. (2020) found that improvements in sewage treatments could lead to changes in the carbon cycle. In fact, carbon cycling changed from a CO_2 source area to a sink area for the atmosphere occurred in Tokyo Bay because of sewage improvement between the 1970s and the 2010s (Kubo and Kanda 2020). The changes in carbon flow resulted from improved water quality because of improved efficiency of sewage treatment and increased STP in the basin, which decreased the amount of labile organic carbon flowing into coastal waters (Kubo et al. 2015; Kubo and Kanda 2020). However, there are few studies available on carbonate parameter data in urbanized coastal waters. It is difficult to cover the carbon cycling in spatial and seasonal variability at the urbanized area, thus resulting in an uncertain estimate of the carbon budget. Therefore, more available data from many systems with sufficient areal and temporal coverage are needed.

2. Study site and Methods

Lake Hamana is a brackish semi-enclosed lake with an area of 70.4 km^2 and an average water depth of approximately 4.8 m. This lake is connected to the open ocean with a narrow entrance. Land use in the watershed of the lake has urbanized/residential areas to the east, agricultural land to the west, and forested land to the northern part of the lake. River discharge from the northern and eastern parts of the lake account for 70% of the total river discharge (Figure 1). In addition, river discharge from the east side is derived from Sanaru Lake, which is one of the most polluted lakes in Japan. In the watershed of Lake Hamana, sewage coverage increased significantly from 57% to 78% between 1995 and 2010. In addition, most STPs conducted advanced sewage treatment. Consequently, nutrient concentrations in the lake decreased significantly between 1995 and 2016 (Kubo et al. 2020). However, the watershed of the lake has the lowest STP coverage rate in the urbanized coastal areas of Japan, which is clarifying the CO_2 budget of the lake will provide effective basic data for predicting the CO_2 budget in urbanized/urbanizing coastal waters.

Daytime observations were conducted monthly at 14 stations in Lake Hamana during 9:00 and 12:00 from October 2017 to September 2019 (Figure 1). Surface water samples were collected using a bucket on the R/V Hamana of the Shizuoka Fisheries Experimental Station (Hamanako Branch) in the daytime observations. At station 4, night-time observations (21:00) were conducted the day before the daytime observations from September 2018 to September 2019 from the bridge using the bucket. After collecting the samples, water temperature and salinity were measured immediately (EC300, YSI nanotech Inc., USA). Then, the water was collected in a 100 mL glass vials with septa and aluminum seals for total alkalinity (TA) and dissolved inorganic carbon (DIC) analyses with 150 μL of $HgCl_2$. The TA and DIC were measured using an auto-burette titrator (ATT-15, Kimoto Denshi Co., Japan) and their values were calibrated against certified reference material (Batch AO; TA=2257.6±0.9 μmol kg^{-1}, and DIC=1987.1±0.68 μmol kg^{-1} from KANSO Technos, Japan). The partial pressure of CO_2 (pCO_2) was calculated using the CO2SYS program (Lewis and Wallace, 1998). Excess DIC (EDIC) was calculated as the difference between the measured DIC concentrations and the theoretical atmospheric equilibrium DIC concentrations following the method of Abril et al. (2003). In addition, DIC and TA of the river water were collected from the bridge using bucket as the land water end-member on the same day as the ship observations (Figure 1). On the other hand, the value of St. 2 at the lake mouth were used for the seaward end-member.

The dissolved oxygen (DO) concentration was measured using the Winkler technique. The apparent oxygen utilization (AOU) was calculated based on the difference between the saturation concentrations and the measured concentrations of DO. Chlorophyll a (Chl a) concentrations were determined using the fluorometric method (Suzuki and Ishimaru 1990). Chemical oxygen demand (COD) was determined by titration with potassium permanganate. Total nitrogen (TN) and total phosphorous (TP) were measured using persulfate oxidation. DO, Chl a, COD, TN and TP samples were not collected in the riverine stations and night-time observations.

The data for precipitation and hours of sunlight were obtained from the Japan Meteorological Agency (https://www.data.jma.go.jp/obd/stats/etrn/index.php).

The principal component analysis (PCA) was applied to identify the controlling factor of pCO_2 using the statistical add-in software XLSTAT (version 2015).

3. Results and Discussion

The surface water temperature and salinity were low in the eastern and northern parts of the lake (stations 5, 6, 10, and 11) and gradually increased in the southern part (station 2) because the eastern and northern part of the lake was connected to the river and the southern part of the lake was connected to the Pacific Ocean (Figure 1, Table 1). Water temperatures were high during spring and summer, while salinity was low during spring and summer (Figure S1). However, the seasonal variation in salinity was not as clear as that of water temperature. An extreme decrease in salinity was observed throughout the lake in May 2018, September 2018, and July 2019. This was due to the increased river flow from the precipitation that had accumulated across five days; it had exceeded 150 mm before the observation.

The TA and DIC concentrations were low in the eastern and northern parts of the lake (stations 5, 6, 10, and 11), which corresponded to the low salinity areas. In contrast, the TA and DIC concentrations gradually increased in the southern part of the lake (stations 1, 2, 3, 4, and 7) in accordance with that of salinity. During the rainfall events (May and September 2018 and July 2019), the TA and DIC concentrations in the entire lake also decreased significantly. Freshwater discharge decreased the TA and DIC concentrations in the lake because river water TA and DIC concentrations (freshwater end-member of the lake) were lower than those of the lake and were 733±125 μmol kg^{-1} (n=6) and 743±120 μmol kg^{-1} (n=6), respectively. A mixing diagram of a TA concentrations and salinity were usually strongly linear which indicates that mixing between freshwater and seawater was conservative. Actually, in the surface water of the lake, relationship between TA and salinity was a linear (Figure 2(a)). In contrast, a mixing diagram of DIC concentrations and salinity at the coastal waters may be conservative (e.g., Bouillon et al. 2007; Paquay et al. 2007) or non-conservative (e.g., Bouillon et al. 2007; Gupta et al. 2008) depending on the area. In the surface water of the lake, DIC showed non-conservative behavior with significant internal consumption (Figure 2(b)) because biological utilization of DIC may be significant at the lake.

The seasonal variations in TA and DIC concentrations are shown in Figure S1. The TA and DIC concentrations were high during November and April and relatively constant (the average TA and DIC concentrations were 2069±252 μmol kg^{-1} and 1854±220 μmol kg^{-1}, respectively). In contrast, they were low during May and October (the TA and DIC concentrations were 1783±347 μmol kg^{-1} and 1535±306 μmol kg^{-1}, respectively).

The pCO_2 values in the daytime of the surface lake water ranged from 29 to 1476 μatm. Across 336 data points, these values indicated that a total of 296 points were undersaturated with respect to the atmospheric equilibrium. In contrast, oversaturated pCO_2 was found only at 40 data points. Although there was no distinct pattern observed for the seasonal variations of pCO_2 at the entire lake, low values were mainly observed stratified seasons from May to September (Figure S1) because of seasonal stratification may lead to higher phytoplankton production and export of organic carbon below the pycnocline (Kone et al., 2009). However, the entire lake was oversaturated in April and September 2018 and July 2019 when heavy rains fell just before the observation, and the rain induced large amounts of terrestrial organic matter into the lake and its decomposition to CO_2. In general, water turbidity is high after rainfall, and phytoplankton activity is low because the photic layer is extremely shallow even at high nutrient concentrations (e.g., Wondie et al. 2007). As a result, the production of CO_2 from organic matter decomposition exceeds the consumption of CO_2. Apart from the observations after rainfall, oversaturated pCO_2 was mainly observed in the eastern part of the lake (stations 4 and 5). Since the eastern part of Lake Hamana is connected to Lake Sanaru, which is one of the most polluted and eutrophicated lakes in Japan, the organic carbon input in this part of Lake Hamana was significantly higher than that of the northern and western parts of the lake. The annual mean concentration of COD in the surface layer of Lake Sanaru (8.2±0.8 mg L^{-1}) was considerably higher than that in Lake Hamana (1.8±0.7 mg L^{-1})

because the sewage system is not well developed and domestic wastewater flow directly into the Lake Sanaru. Therefore, the pCO_2 was mainly oversaturated at the east side of the lake because of the CO_2 produced from organic matter inflow and decomposition.

At station 4, the pCO_2 values in the night-time ranged from 187 to 597 μatm during September 2018 and September 2019. The averaged value of pCO_2 was 361.5±104.3 μatm (Figure 3). In contrast, the pCO_2 values in the daytime ranged from 290 to 555 μatm. The averaged value of pCO_2 was 373.5±100.4 μatm during same observation periods. The pCO_2 values observed in the night-time were often higher than those observed in the daytime, but the difference was not significant ($p>0.05$ Mann-Whitney test). Similarly, salinity was also higher in the daytime, but not significant ($p>0.05$ Mann-Whitney test). In addition, the observation that was undersaturated pCO_2 in the daytime and oversaturated in night-time was only in April 2019. Although the night-time pCO_2 was affected by biological respiration, the conclusion that Lake Hamana is an undersaturated pCO_2 area is not likely to change significantly. Similarly, no significant difference was found in the relatively high salinity area (>30) in Tokyo Bay and Guanabara Bay which are undersaturated pCO_2 areas with very high primary production (Cotovicz et al. 2015, Kubo et al. 2017). However, in this study, since the duration and number of observations are limited in the night-time observation, more detailed observations are needed to estimate the CO_2 budget of the entire Lake Hamana.

The DO saturation ratio (DO%) of the surface lake water ranged from 73 to 191% (108±19%). Of the total 288 data points for DO%, 186 of them were oversaturated with respect to the atmospheric equilibrium. There was a significant negative correlation between pCO_2 and DO% overall (Figure 4, $R^2=0.45$, $p<0.001$, $n=288$). Therefore, active photosynthesis was the main factor that controlled pCO_2 in the lake because pCO_2 was undersaturated and DO was oversaturated. In the low salinity area (<25), Chl a concentrations were very high and pCO_2 was low (<200 μatm). In contrast, in the high salinity area (>25), concentrations of Chl a were slightly low, and pCO_2 was nearly at atmospheric equilibrium (200–400 μatm). The DO% was lowest in the eastern part of the lake (station 3: 97±8% and station 4: 95±8%). These variations were inversely correlated with those of pCO_2 in the eastern part of the lake ($p<0.0001$). Therefore, the oversaturation of pCO_2 in the eastern part of the lake was derived from terrestrial organic carbon input and degradation.

There was a significant positive relationship between EDIC and AOU overall according to the equation below (Figure 5):

$$[EDIC]= (1.10 \pm 0.06) \times [AOU] - 47 \pm 3 \quad (R^2=0.56,\ p<0.001,\ n=288) \qquad (1)$$

The line with slope 1 (Figure 5: dashed red line) represents the quotient between CO_2 and O_2 during primary production and community respiration (Borges and Abril 2011; Cotovicz et al. 2015). The slope of EDIC and AOU was 1.10±0.06 in Lake Hamana, which was largely dominated by a strong biological effect of the primary production and consumption of CO_2. In addition, EDIC was mostly negative in Lake Hamana, suggesting that CO_2 was consumed by primary production. In many cases, the AOU values were closer to zero than the EDIC values. These results indicate a more rapid equilibration of O_2 rather than CO_2 (Borges and Abril 2011). There was a possibility that the high primary production in the lake derived from effluents from sewage treatment plants, which was low carbon and high nitrogen. Kubo et al. (2020) indicated that carbon/nitrogen ratio of STP effluents was low at the watershed of the lake because insufficient of denitrification at the STPs. The intercept of the regression line was −47±3 and many values were below the 1:1 line, suggesting a negative EDIC. This may be inflow of undersaturated CO_2 water supply from open ocean (Tokoro et al., 2021). Alternatively, the consumption of DIC from calcium carbonate production is also possible (Borges and Abril 2011), but this contribution was not investigated in this study.

A PCA was conducted to determine the variable contribution of the total data of daytime pCO_2, DO%, Chl a, salinity, temperature, COD, sum of previous and observations day's sunlight hours, and 3 days of accumulated precipitation. The PCA results also suggested a strong biological effect on the dynamics of pCO_2 in Lake Hamana (Figure 6(a)). Factor 1 explained 42% of the total variance, revealing that pCO_2 was negatively related to Chl a, COD, and DO%. Indeed, high phytoplankton activity produces organic matter and DO. The positive correlation between Chl a and COD in Lake Hamana indicates that the contribution of phytoplankton activities in the lake is large. In contrast, negative correlations between COD and salinity indicates the influence of organic matter inflow from the land. To clarify the findings obtained from this study in more detail, it is necessary to observe organic carbon isotope ratios and determine the quantitative contribution of each source, because isotope analysis enables the identification of organic carbon sources (e.g., Watanabe and Kuwae, 2015; Kubo and Kanda, 2020). In contrast, the PCA revealed that pCO_2 was weakly related to meteorological data (sunlight hour and precipitation), although high pCO_2 was observed after heavy rain. Therefore, the PCA was conducted to determine the variable contribution of the data at stations 3, 4, and 5 in the river mouth stations. The results of the PCA suggested moderate meteorological control on the dynamics of pCO_2 in the eastern part of the lake (Figure 6(b)). Factor 2 explained 27.9% of the total variance, revealing that

pCO_2 was positively related to precipitation, although there was no correlation between Chl a and COD. Therefore, the oversaturation of pCO_2 with respect to the atmospheric equilibrium at the river mouth stations was due to the increase in the supply and decomposition of terrestrial organic carbon.

From the above results, it can be concluded that, although CO_2 is generated by the decomposition of organic matter from terrestrial sources on the east side of the lake, the entirety of Lake Hamana is a net sink for CO_2 because of its active phytoplankton activities.

In the watershed of Lake Hamana, the STP coverage rate is approximately 78%, which is the lowest for urbanized coastal waters in Japan. In contrast, in the watershed of Osaka Bay, Tokyo Bay, and Ise Bay in highly urbanized coastal waters in Japan, which have been reported to be significant net CO_2 sink areas (Fujii et al. 2013; Endo et al. 2017; Kubo et al. 2017; Tokoro et al. 2021), the STP coverage rate is almost 100%. These waters are considered to be sink areas with relatively high nutrient inflow compared to organic carbon inflow (Kuwae et al. 2016; Kubo et al. 2019; Kubo and Kanda 2020). Concentrations of COD in Tokyo Bay and Lake Hamana in 2013 were 2.9 and 1.9 mg L^{-1}, respectively (Kubo et al., 2020; Ando et al., 2021). In contrast, DIN and PO_4^{3-} concentrations were 17.5 and 0.7 μmol L^{-1} in Tokyo Bay (Kubo et al., 2019) and were 3.9 and 0.1 μmol L^{-1} in Lake Hamana in 2013 (Kubo et al., 2020). COD/DIN and COD/PO_4^{3-} ratio were 0.17 and 4.1 in Tokyo Bay, were 0.49 and 19 in Lake Hamana. Although nutrient concentrations were higher in Tokyo Bay than in Lake Hamana, COD/DIN and COD/PO_4^{3-} ratio were lower in Tokyo Bay, indicating that nutrient were relatively more abundant than organic carbon in Tokyo Bay. However, these ratios in Tokyo Bay and Lake Hamana are much smaller than those of other coastal waters where STP coverage was low, and CO_2 emitted to the atmosphere (COD/DIN>100, COD/PO_4^{3-}>4400; Ran et al., 2015, Shen et al., 2015). Therefore, the CO_2 sinks in both coastal areas are considered to be the result of the removal of labile organic carbon by STP. In addition, Lake Hamana and the above-mentioned Japanese coastal waters where CO_2 uptake has been reported were marine-dominated estuaries, which was defined by Jiang et al. (2009). Jiang et al. (2009) reported that marine-dominated estuaries were weaker emitters of CO_2 to the atmosphere than river-dominated estuaries because the contribution of organic carbon was small. Therefore, in marine-dominated and urbanized coastal waters with STP, such as the coast of Japan, there is a possibility of shifting from weaker CO_2 source areas to CO_2 sink areas. In the future, coastal waters around the world will be covered with STP; as the maintenance rate increases, continuous observations of the CO_2 budget will allow for a more detailed assessment of CO_2 changes in urban coastal waters.

Acknowledgments

We would like to thank the crew members on board the R/V Hamana for their help with sampling. This work was supported by a Grant-in-Aid for Young Scientists (19K20436) from the Ministry of the Education, Culture, Sports, Science and Technology, Japan to A.K.

Declaration of interests

The authors declare that they have no known competing financial interests or personal relationships that could have appeared to influence the work reported in this paper.

References

Abril G, Etcheber H, Delille B, Frankignoulle M, Borges AV (2003) Carbonate dissolution in the turbid and eutrophic Loire estuary. Marine Ecology Progress Series 259: 129-138.

Ando H, Maki H, Kashiwagi N, Ishii Y (2021) Long-term change in the status of water pollution in Tokyo Bay: recent trend of increasing bottom-water dissolved oxygen concentrations. Journal of Oceanography doi: http://doi.org/10.1007/s10872-021-00612-7.

Borges AV, Abril G (2011) Caron dioxide and methane dynamics in estuaries. In: Wolanski E McLusky DS (eds.). Treatise on Estuarine and Coastal Science. 5. pp.119-161. Waltanm: Academic Press.

Bouillon S, Dehairs F, Velimirov B, Abril G, Borges AV (2007) Dynamics of organic and inorganic carbon across contiguous mangrove and seagrass systems (Gazi Bay, Kenya). Journal of Geophysical Research 112: G02018.

Brauko KM et al. (2020) Marine heatwaves, sewage and eutrophication combine to trigger deoxygenation and biodiversity loss: A SW Atlantic case study. Frontiers in Marine Science 7: 590258.

Breitburg D et al. (2018) Declining oxygen in the global ocean and coastal waters. Science 359: eaam7240

Chen CTA, Borges AV (2009) Reconciling opposing views on carbon cycling in the coastal ocean: Continental shelves as sinks and near-shore ecosystems as sources of atmospheric CO_2. Deep Sea Research II 56: 578-590.

Chen CT et al. (2013) Air-sea exchanges of CO_2 in the world's coastal seas. Biogeosciences 10: 6509-6544.

Coma R et al. (2009) Global warming-enhanced stratification and mass mortality events in the Mediterranean Proceedings of the National Academy of Sciences of the United States of America 106: 6176-6181.

Cotovicz Jr LC, Knoppers BA, Brandini N, Costa Santos SJ, Abril G (2015) A strong CO_2 sink enhanced by eutrophication in a tropical coastal embayment (Guanabara Bay, Rio de Janeiro, Brazil). Biogeosciences 12: 6125-6146.

Cotovicz Jr LC, Knoppers BA, Deirmendjian L, Abril G (2019) Sources and sinks of dissolved inorganic carbon in an urban tropical coastal bay revealed by δ^{13}C-DIC signals. Estuarine, Coastal and Shelf Science 220: 185-195.

Endo T, Shimano J, Harada N, Sakai D, Fujiwara R (2017) Relationship between vertical distribution of pCO_2 in sea and air-sea CO_2 exchange in inner part of Osaka Bay. Journal of Japan Society of Civil Engineers (B2: Coastal Engineering) 73: I_1231-I_1236.

Frankignoulle M et al. (1998) Carbon dioxide emission from European estuaries. Science 282: 434-436.

Fujii T, Fujiwara T, Nakayama K (2013) Fluxes of carbon dioxide in the eastern regions of Osaka Bay. Japan Society of Civil Engineers (B2) 69:1111–1115 (in Japanese with English abstract).

Gupta GVM et al. (2008) Influence of net ecosystem metabolism in transferring riverine organic carbon to atmospheric CO_2 in a tropical coastal lagoon (Chilka Lake, India). Biogeochemistry 87: 265-285.

Hotchkiss ER et al. (2015) Sources of and processes controlling CO_2 emissions change with the size of streams and rivers. Nature Geoscience 8: 696-699.

Jiang LQ, Cai WJ, Wang Y (2009) A comparative study of carbon dioxide degassing in river- and marine-dominated estuaries. Limnology and Oceanography 53: 2603-2615.

Koné YJM, Abril G, Kouadio KN, Delille B, Borges AV (2009) Seasonal variability of carbon dioxide in the rivers and lagoons of Ivory Coast (West Africa). Estuaries and Coasts 32: 246-260.

Kubo A, Yamamoto-Kawai M, Kanda J (2015) Seasonal variations in concentration and lability of dissolved organic carbon in Tokyo Bay. Biogeosciences 12: 269–279.

Kubo A, Maeda Y, Kanda J (2017) A significant net sink for CO_2 in Tokyo Bay. Scientific Reports 7: 44355.

Kubo A, Hashihama F, Kanda J, Horimoto-Miyazaki N, Ishimaru T (2019) Long-term variability of nutrient and dissolved organic matter concentrations in Tokyo Bay between 1989 and 2015. Limnology and Oceanography 64: S209-S222.

Kubo A, Kanda J. (2020) Coastal urbanization alters carbon cycling in Tokyo Bay. Scientific Reports 10: 20413.

Kubo A, Imaizumi R, Yamauchi S (2020) Lake water phosphate reduction with advanced wastewater treatment in watershed, at Lake Hamana, Shizuoka Prefecture, Japan, from 1995 to 2016. Environmental Science and Pollution Research 27: 2120-2130.

Kuwae T et al. (2017) CO_2 uptake in the shallow coastal ecosystems affected by anthropogenic impacts. In: Kuwae T, Hori M (eds.). Blue Carbon in Shallow Coastal Ecosystems. pp. 295-319. Springer Singapore.

Kuwae T et al. (2016) Blue carbon in human-dominated estuarine and shallow coastal systems. Ambio 45: 290-301.

Lewis E, Wallace D (1998) Program developed for CO_2 system calculations. Carbon dioxide information analysis center, Oak Ridge National Laboratory, U.S. Department of Energy, Oak Ridge, Tennessee.

Li Y et al. (2020) The spatiotemporal variation and control mechanism of surface pCO_2

in winter in Jiaozhou Bay, China. Continental Shelf Research 206: 104208.

Liu XY, Yang XF, Li YX, Zhang LJ (2019) Sea surface pCO_2 in an urbanized coastal system (Jiaozhou Bay, China) during summer. Marine Pollution Bulletin 146: 767-778.

Paquay FS, Mackenzie FT, Borges AV (2007) Carbon dioxide dynamics in rivers and coastal waters of the "big island" of Hawaii, USA, during baseline and heavy rain conditions. Aquatic Geochemistry 13: 1-18.

Ran L, Lu XX, Richey JE, Sun H, Han J, Yu R, Liao S, Yi Q (2015) Long-term spatial and temporal variation of CO_2 partial pressure in the Yellow River, China. Biogeosciences 12: 921-932.

Shen X, Sun T, Liu F, Xu J, Pang A (2015) Aquatic metabolism response to the hydrologic alteration in the Yellow River estuary, China. Journal of Hydrology 525: 42-54.

Suzuki R, Ishimaru T (1990) An improved method for the determination of phytoplankton chlorophyll using N, N-Dimethylformamide. Journal of the Oceanographical Society of Japan 46: 190-194.

Tokoro et al. (2021) Contribution of biological effects to carbonate-system variations and the air-water CO_2 flux in urbanized bays in Japan. Journal of Geophysical Research Oceans 12: e2020JC016974. DOI: https://doi.org/10.1002/essoar.10505162.1.

Watanabe K, Kuwae T (2015) How organic carbon derived from multiple sources contributes to carbon sequestration processes in a shallow coastal system? Global Change Biology 21: 2612-2623.

Wondie A, Mengistu S, Vijverberg J, Dejen E (2007) Seasonal variation in primary production of a large high altitude tropical lake (Lake Tana, Ethiopia): effects of nutrient availability and water transparency. Aquatic Ecology 41: 195-207.

Availability of data and materials

All data generated or analyzed during this study are included in this published article and its supplementary information files.

Funding

This work was supported by a Grant-in-Aid for Young Scientists (19K20436) from the Ministry of the Education, Culture, Sports, Science and Technology, Japan to A.K.

Author information

Affiliations

Atsushi Kubo, Keisuke Yoshida, Kei Suzuki

Department of Geosciences, Shizuoka University, 836 Ohya, Suruga-ku, Shizuoka, 422-8529, Japan

Author contributions

A.K. conceived this study. All authors conducted field observations, sample analysis, and data analysis. A. K. wrote the initial draft.

Corresponding author

Correspondence to Atsushi Kubo.

Ethics declarations

Ethics approval and consent to participate

Not applicable

Consent to publication

Not applicable

Competing interests

The authors declare that they have no competing interests.

Figure 1. Map of Lake Hamana. Black circles and stars indicate sampling lake stations and river stations, respectively.

Figure 2. (a) TA and (b) DIC against salinity for all samples. Red dashed lines indicate the hypothetical conservative mixing line between TA or DIC and salinity.

Figure 3. (a) Salinity and (b) pCO_2 variations of daytime (about 9:00) and night-time (about 21:00) at station 4. Blue and gray indicate daytime and night-time observations, respectively.

Figure 4. (a) DO%–pCO_2–Salinity and (b) DO%–pCO_2–Chl a relationship. The color of plot indicates (a) Salinity and (b) Chl a, respectively.

Figure 5. Relationship between apparent oxygen utilization (AOU) and excess DIC (EDIC). Black and gray dashed lines indicate linear regression and 95% confidence interval lines, respectively. Red dashed line indicates a 1:1 line, which represents the quotient between CO_2 and O_2 during the processes of photosynthesis and respiration.

Figure 6. Principal component analysis (PCA) based on (a) total data and (b) data at the eastern side of the lake (station 3, 4, and 5) for sampling campaign using the data of pCO_2, DO%, Chl a, salinity, temperature, COD, sunlight hour, and 3 days of accumulated precipitation.

Table 1. Data of each parameter (mean±standard deviation, minimum, and maximum) at

all stations.

Table 2. Data of each parameter (mean±standard deviation, minimum, and maximum) at all stations.

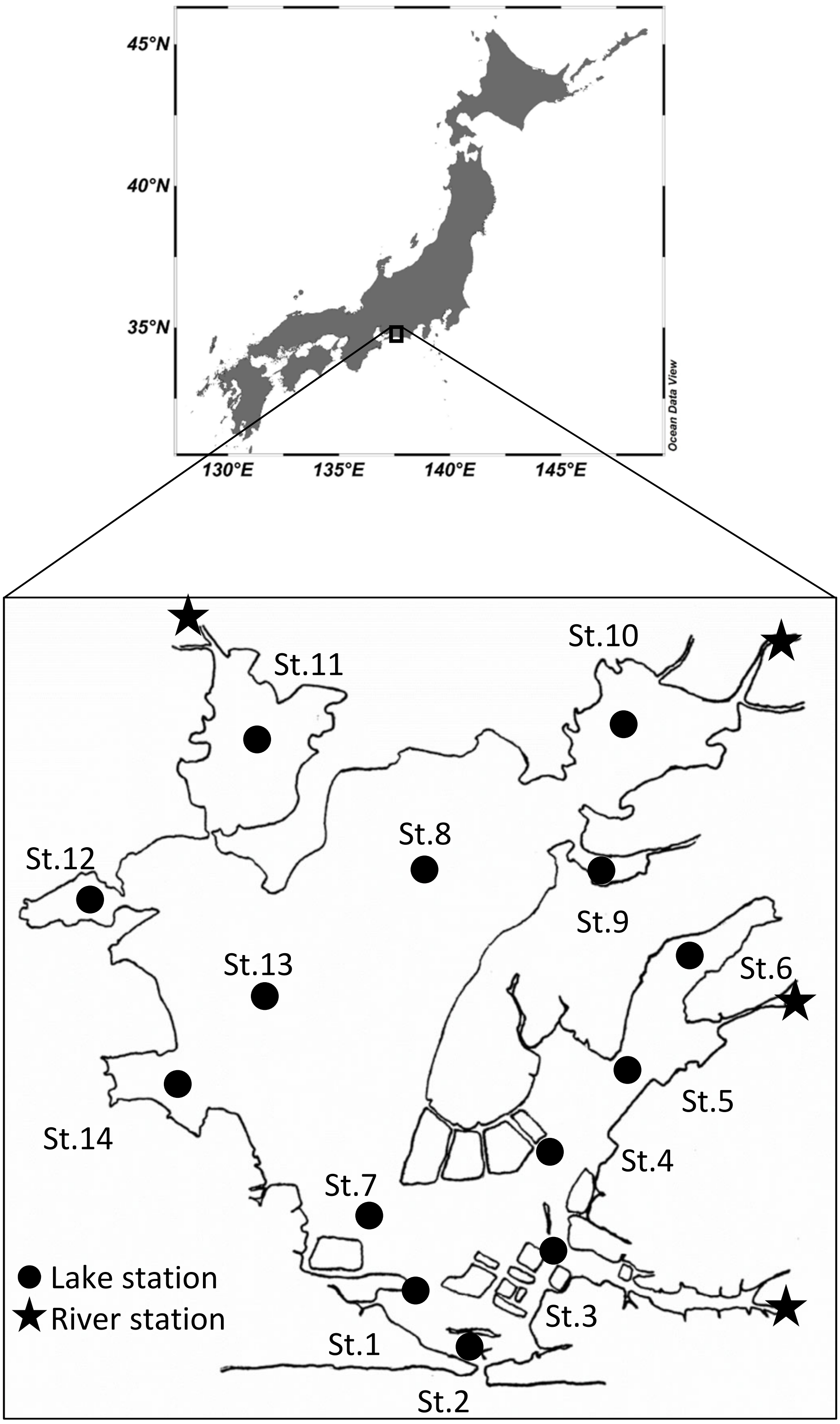

Figure 1. Map of Lake Hamana. Black circles and stars indicate sampling lake stations and river stations, respectively.

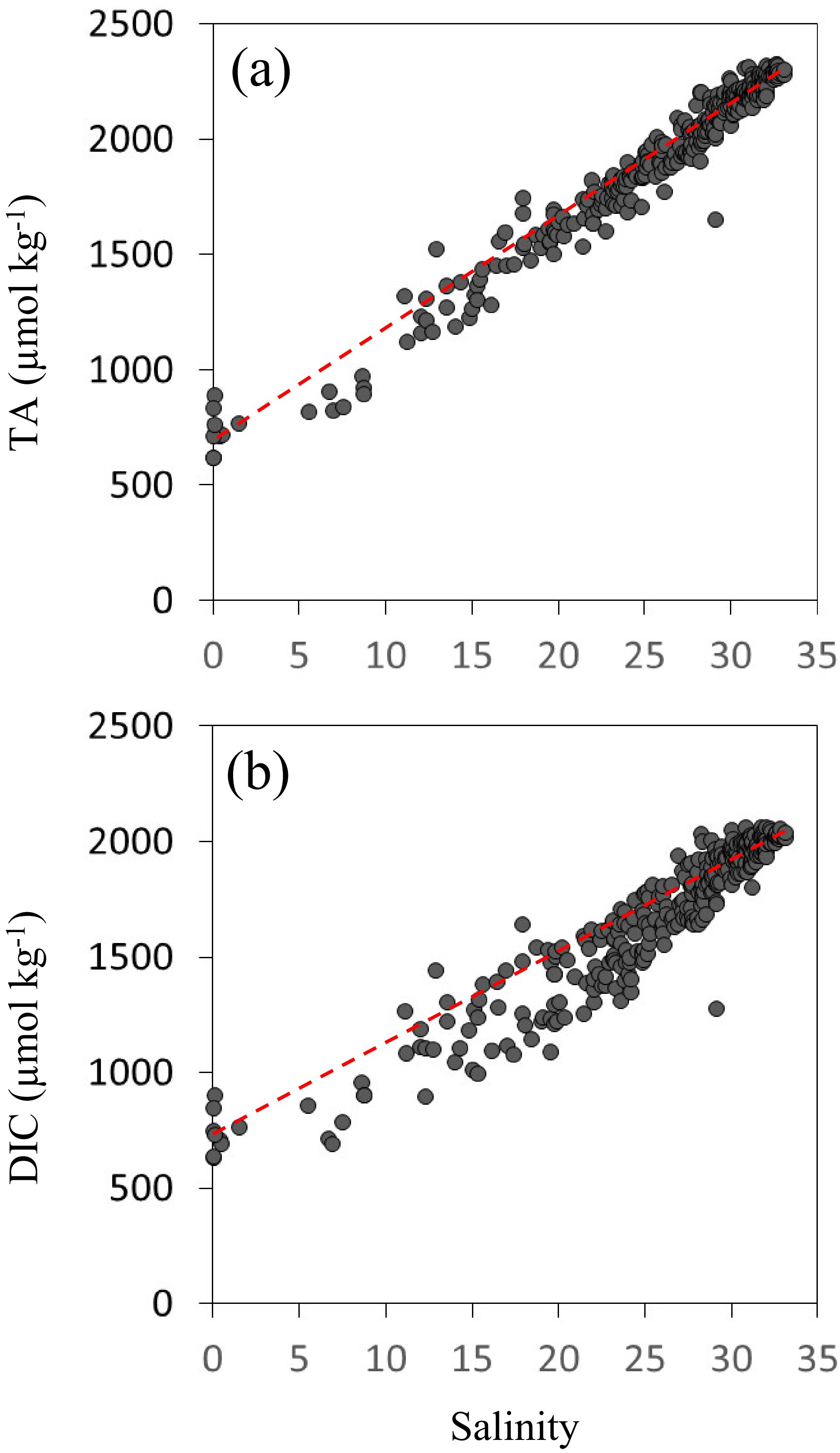

Figure 2. (a) TA and (b) DIC against salinity for all samples. Red dashed lines indicate the hypothetical conservative mixing line between TA or DIC and salinity.

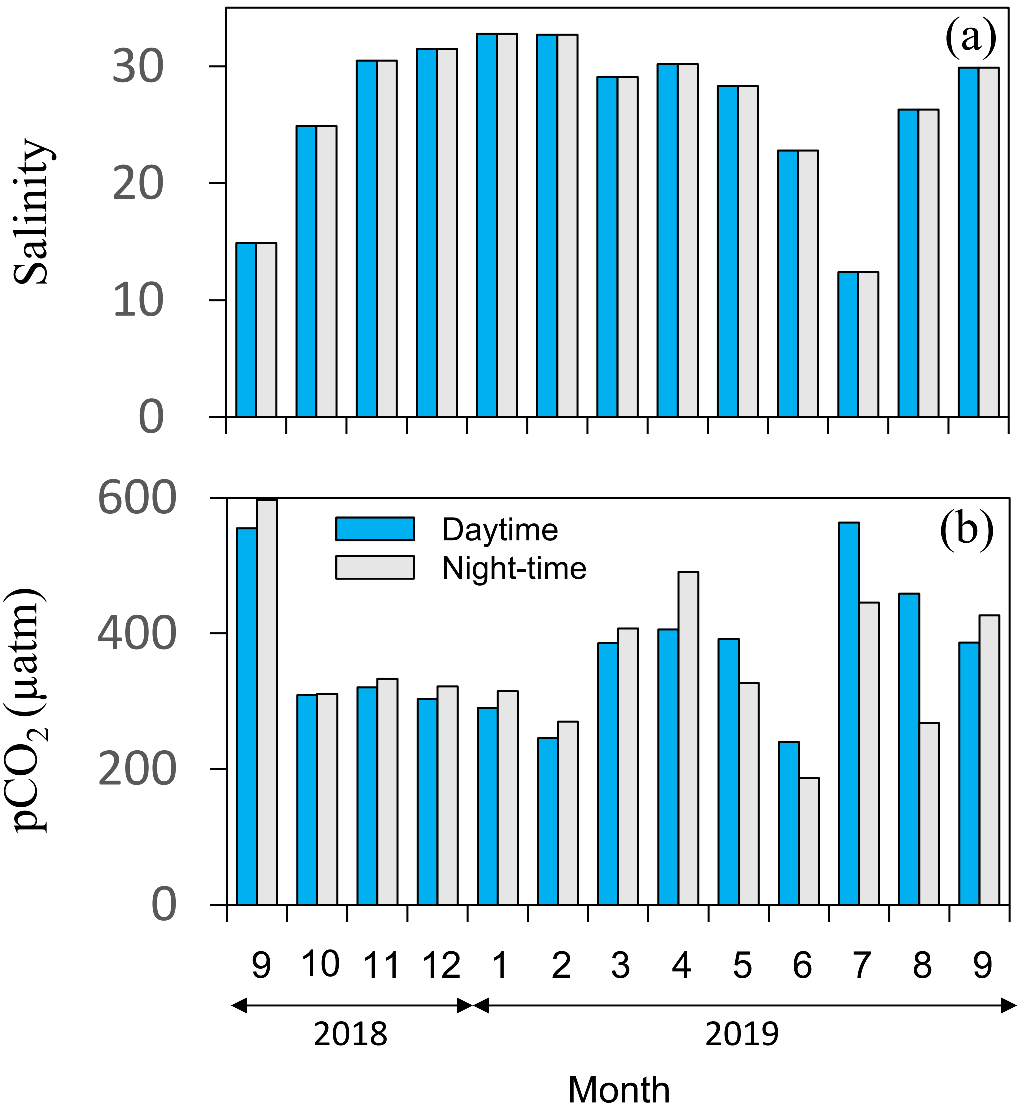

Figure 3. (a) Salinity and (b) pCO2 variations of daytime (about 9:00) and night-time (about 21:00) at station 4. Blue and gray indicate daytime and night-time observations, respectively.

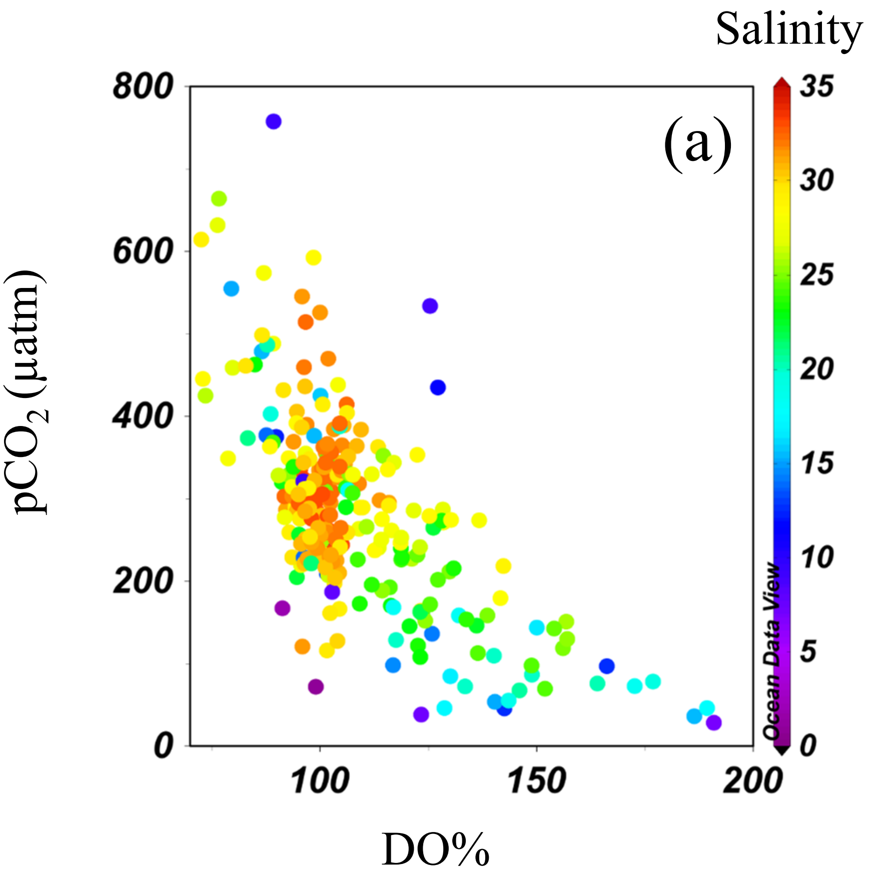

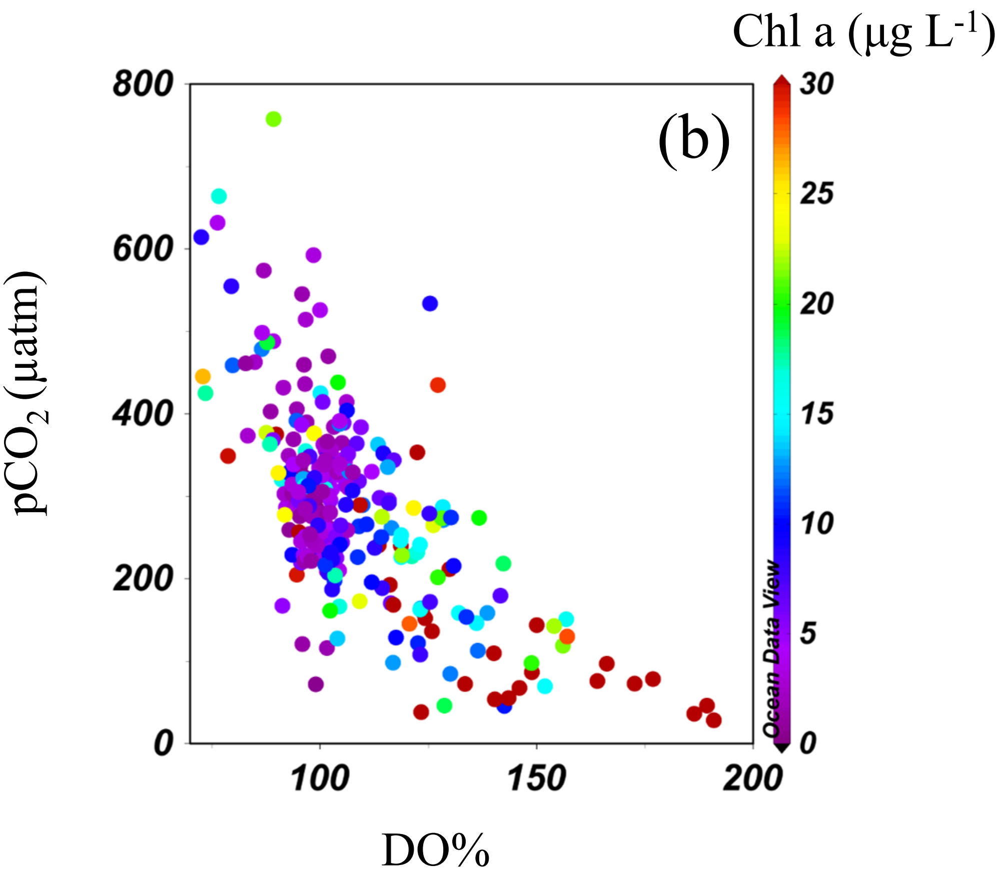

Figure 4. (a) DO%–pCO2–Salinity and (b) DO%–pCO2–Chl a relationship. The color of plot indicates (a) Salinity and (b) Chl a, respectively.

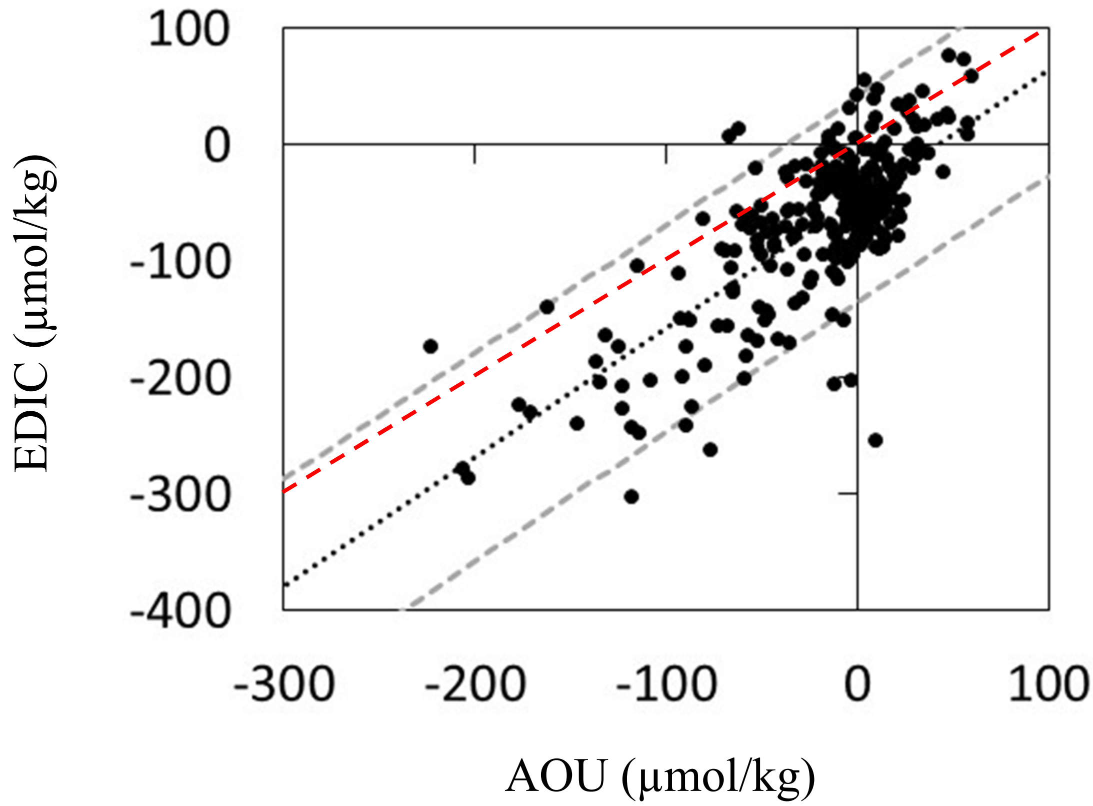

Figure 5. Relationship between apparent oxygen utilization (AOU) and excess DIC (EDIC). Black and gray dashed lines indicate linear regression and 95% confidence interval lines, respectively. Red dashed line indicates a 1:1 line, which represents the quotient between CO2 and O2 during the processes of photosynthesis and respiration.

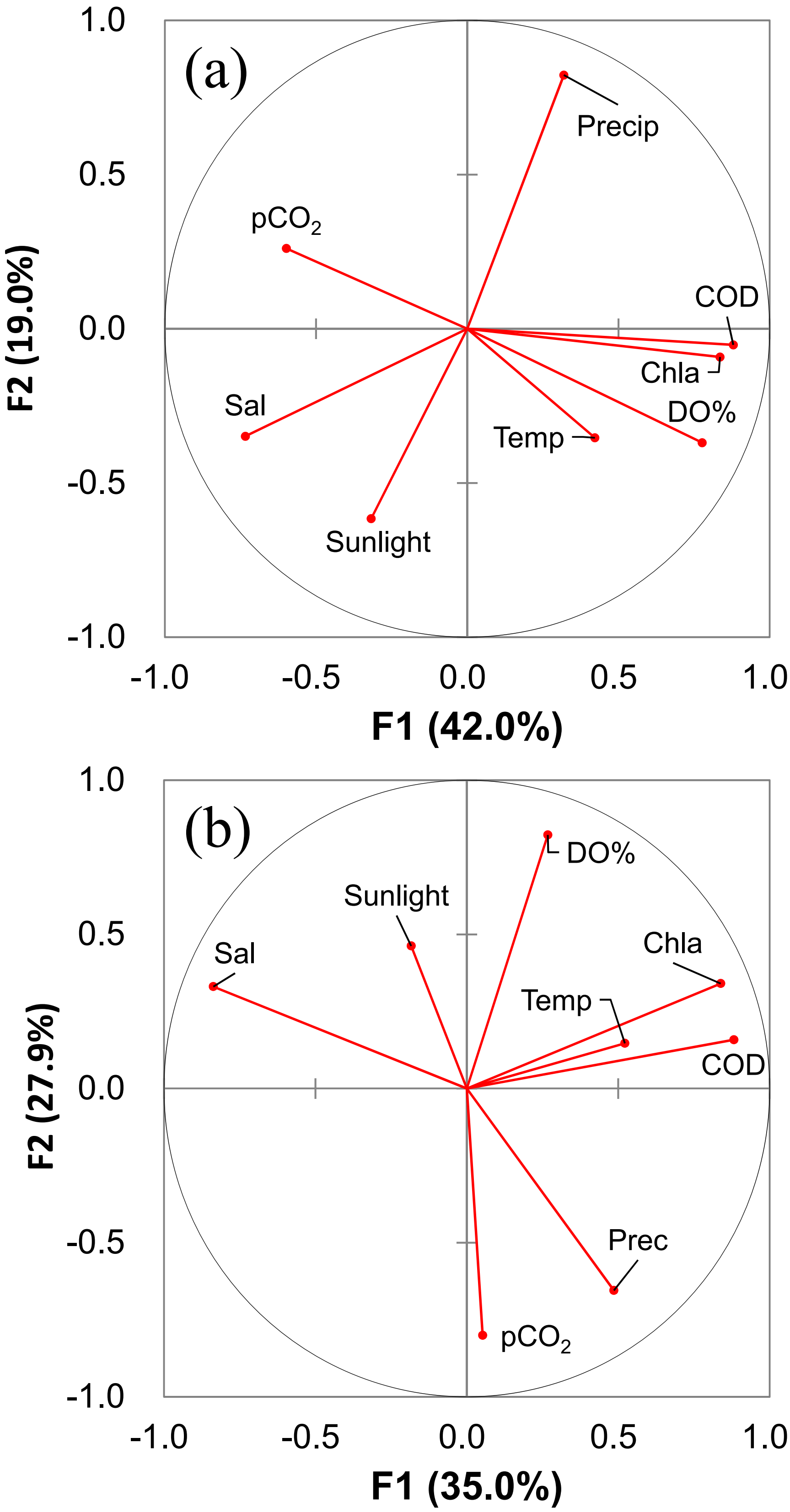

Figure 6. Principal component analysis (PCA) based on (a) total data and (b) data at the eastern side of the lake (station 3, 4, and 5) for sampling campaign using the data of pCO2, DO%, Chl a, salinity, temperature, COD, sunlight hour, and 3 days of accumulated precipitation.

Table 1
Data of each parameter (mean±standard deviation, minimum, and maximum) at all stations.

Station	Temperature (°C)	Salinity	TA (μmol kg^{-1})	DIC (μmol kg^{-1})	pCO_2 (μatm)
1	19.5±6.2 (6.5-29.8)	29.6±2.7 (21.8-32.8)	2139±180 (1647-2307)	1871±189 (1271-2054)	296±83 (116-488)
2	19.7±5.4 (10.8-29.5)	31.1±2.3 (22.6-33.2)	2196±130 (1750-2317)	1933±104 (1605-2055)	328±66 (248-615)
3	19.4±6.1 (6.4-30.3)	28.4±5.5 (12.1-33.1)	2057±292 (1228-2314)	1837±225 (1183-2040)	353±88 (252-664)
4	18.9±6.9 (5.8-31.1)	27.6±5.0 (13.6-32.8)	1980±287 (1218-2315)	1777±235 (1175-2018)	345±81 (240-555)
5	17.9±8.4 (4.3-31.8)	22.4±6.3 (8.8-29.8)	1697±350 (888-2126)	1529±316 (893-1938)	311±162 (129-758)
6	18.3±8.8 (4.6-32.5)	20.8±5.0 (5.6-27.4)	1635±278 (813-2078)	1456±240 (854-1840)	334±294 (51-1476)
7	19.5±6.2 (7.0-30.7)	30.1±3.1 (20.6-32.8)	2129±181 (1621-2316)	1875±167 (1478-2052)	314±71 (173-470)
8	18.6±8.0 (6.0-31.9)	26.7±5.4 (8.7-32.1)	1952±290 (965-2259)	1699±281 (950-2025)	253±104 (72-534)
9	18.4±8.4 (5.3-32.5)	25.1±4.6 (11.3-30.8)	1890±243 (1118-2196)	1657±239 (1077-2014)	258±109 (74-460)
10	18.5±8.3 (5.6-32.9)	20.0±9.1 (0.5-30.2)	1683±438 (705-2169)	1503±377 (685-1969)	255±121 (72-593)
11	18.6±8.4 (5.3-32.7)	22.8±8.0 (6.8-31.4)	1742±440 (816-2241)	1496±434 (685-2014)	192±120 (29-526)
12	18.5±8.2 (5.4-32.0)	26.7±5.1 (15.1-32.1)	1930±292 (1258-2252)	1678±317 (989-2021)	240±106 (36-514)
13	18.6±7.9 (6.3-31.3)	27.5±3.9 (19.2-32.0)	1986±213 (1575-2261)	1721±245 (1235-2034)	242±94 (68-415)
14	18.6±8.1 (5.8-31.9)	27.1±4.2 (17.5-31.7)	1946±233 (1454-2225)	1692±280 (1075-2015)	250±113 (46-545)

Table 2

Data of each parameter (mean±standard deviation, minimum, and maximum) at all stations.

Station	DO%	Chla (μg L^{-1})	COD (mg L^{-1})	TN (mg L^{-1})	TP (mg L^{-1})
1	100±8 (92-121)	5.2±6.6 (0.4-29.3)	1.3±0.3 (0.7-1.8)	0.16±0.07 (0.05-0.35)	0.018±0.007 (0.010-0.038)
2	100±7 (73-116)	3.8±4.1 (0.2-16.3)	1.3±0.3 (0.9-1.9)	0.16±0.09 (0-0.43)	0.020±0.013 (0.010-0.059)
3	97±8 (77-110)	6.8±8.4 (0.4-39.6)	1.6±0.4 (1.1-2.4)	0.28±0.19 (0.05-0.73)	0.034±0.030 (0.011-0.130)
4	95±8 (80-119)	7.5±8.5 (0.5-34.6)	1.5±0.4 (0.9-2.6)	0.33±0.21 (0.10-0.88)	0.035±0.027 (0.011-0.130)
5	102±17 (73-139)	17.6±16.2 (0.9-54.0)	2.0±0.5 (1.2-3.0)	0.75±0.44 (0.27-1.90)	0.054±0.040 (0.021-0.200)
6	No Data	27.8±21.4 (2.3-91.0)	No Data	No Data	No Data
7	103±8 (83-122)	5.4±5.8 (0.7-22.8)	1.4±0.4 (0.8-2.1)	0.19±0.09 (0.05-0.48)	0.020±0.010 (0.011-0.046)
8	115±17 (96-173)	11.1±9.5 (1.9-39.2)	1.9±0.6 (1.1-3.3)	0.28±0.14 (0.11-0.79)	0.029±0.026 (0.008-0.120)
9	No Data	14.1±11.6 (1.2-37.7)	No Data	No Data	No Data
10	113±20 (89-166)	13.8±14.0 (0.4-62.7)	1.8±0.5 (1.0-2.9)	0.52±0.34 (0.18-1.50)	0.036±0.021 (0.011-0.098)
11	120±24 (96-191)	18.9±18.1 (1.5-67.3)	2.4±1.0 (1.1-5.2)	0.83±0.77 (0.21-3.10)	0.040±0.030 (0.011-0.120)
12	118±24 (79-186)	19.1±21.1 (2.4-85.1)	2.0±0.6 (1.0-3.7)	0.37±0.27 (0.13-1.20)	0.030±0.031 (0.007-0.160)
13	113±20 (88-177)	10.4±10.2 (1.2-43.9)	1.8±0.5 (1.1-3.0)	0.26±0.11 (0.14-0.58)	0.021±0.012 (0.009-0.055)
14	117±25 (73-189)	20.1±25.5 (1.1-117.6)	2.1±1.2 (1.0-7.1)	0.39±0.34 (0.14-1.90)	0.039±0.056 (0.010-0.300)